CLIMATE

Abrupt cloud clearing of marine stratocumulus in the subtropical southeast Atlantic

Sandra E. Yuter[1]*, John D. Hader[1,2], Matthew A. Miller[1], David B. Mechem[3]

We document rapid and abrupt clearings of large portions of the subtropical marine low cloud deck that have implications for the global radiation balance and climate sensitivity. Over the southeast Atlantic, large areas of stratocumulus are quickly eroded, yielding partial or complete clearing along sharp transitions hundreds to thousands of kilometers in length that move westward at 8 to 12 meters per second and travel as far as 1000+ kilometers from the African coast. The westward-moving cloudiness reductions have an annual peak in occurrence in the period from April through June. The cloud erosion boundaries reduce cloud at ≈10-kilometer scale in less than 15 minutes, move approximately perpendicular to the mean flow, and are often accompanied by small-scale wave features. Observations suggest that the cloud erosion is caused by atmospheric gravity waves.

The areal extent and temporal variability of subtropical marine low clouds strongly influence the global radiation balance (*1*). Large, persistent areas of subtropical marine stratocumulus clouds have been called Earth's "climate refrigerator" (*2*). These low marine clouds scatter solar radiation back to space and emit thermal radiation at a temperature close to the sea surface temperature (SST), yielding net radiative cooling of the climate system. The controls on areal coverage of marine stratocumulus have historically been cast either as a steady-state response to an imposed large-scale mean forcing (e.g., SST, subsidence, inversion strength, and radiative flux) (*3*, *4*) or as being dominated by internal aerosol-cloud-precipitation processes (*5*–*7*). Most previous work on low marine cloudiness transitions, including several studies addressing pockets of open cells, has predominantly used frameworks that focus on responses to SST gradients and/or internal aerosol-cloud-precipitation processes and implicitly exclude external multiday synoptic variability (*8*, *9*). Yet a recent spectral analysis of multiyear global satellite datasets (*10*) found that cloudiness variance at multiday (3 to 50 days) time scales exceeds the seasonal variance over the subtropical southeast Atlantic and northeast Pacific and is only slightly lower than the seasonal magnitude over the subtropical southeast Pacific. Abrupt changes in regional albedo from 0.9 (mostly low cloud cover) to 0.6 (ocean under mostly clear sky) will substantially increase the shortwave radiation absorbed by the ocean, which has pronounced implications for marine ecology and biogeochemistry (*11*).

Cloudiness transition boundaries hundreds to thousands of kilometers long in the southeast Atlantic exhibit abrupt reductions of cloud akin to pulling away a sun shade (Fig. 1 and movies S1 to S4). The information below is derived from 377 cloud erosion boundaries, identified from an examination of 1911 days over the period from 8 May 2012 through 31 July 2017 by using moderate resolution imaging spectroradiometer (MODIS) corrected reflectance data and geosynchronous satellite visible and infrared (IR) data (see methods for details). The cloud-eroding events in the southeast Atlantic occur year-round, with a peak monthly frequency of occurrence of roughly 20 events per month in May (Fig. 2). The abrupt cloudiness transitions, up to 1000+ km in meridional length, move westward at 8 to 12 m s^{-1} from 11°E to as far as 4°W longitude, as much as 1500 km from the African coastline (Fig. 3). For any single cloudiness boundary, the speed of motion is relatively constant as the boundary moves westward (Fig. 3). At different locations along the same boundary, cloud reduction can result in partial or complete clearing (Fig. 1). Cloudiness transitions typically become discernible along the coast of southwestern Africa, generally within a few hours of local midnight (Fig. 3 and movies S2 and S4). The removal of cloud at night indicates that shortwave radiation–cloud feedbacks are not required. The prevailing winds at cloud level in this region are typically southerly or southeasterly (*12*), and individual features in the low cloud field can be tracked moving northward relative to the westward-moving cloud erosion boundary (movie S1). The motion of the cloud erosion boundary is roughly perpendicular to the cloud-level winds and cannot be explained primarily by advection.

High-resolution imagery of areas along the cloudiness boundaries often show a sharp and abrupt transition from overcast to clear or from overcast to broken clouds over spatial scales of ≤10 km (Fig. 1). Along some cloudiness boundaries, individual closed cells within the mesoscale cellular structure of the marine stratocumulus appear to be bisected (Fig. 1, F and G). Animated loops of visible satellite imagery reveal that cloud cover over ≈10-km horizontal scales is removed or reduced in 15 min or less (movies S1 and S3). Near the cloud erosion boundaries, sets of wavelike, narrow (wavelength ≤ 10 km), elongated, banded features roughly parallel to the cloudiness boundaries frequently occur (Fig. 1, E and G).

Globally, satellite imagery reveals a rich array of multiday marine low-cloudiness variations, including sharp transitions between areas with nearly overcast and nearly clear conditions. Some of these cloudiness transition boundaries are associated with the advection of low-level air from poleward extratropical cyclones into the subtropics (*13*–*15*). Cloud coverage, type, and height in the midlatitudes are clearly modulated by synoptic-scale baroclinic weather systems (*16*–*18*). Some subtropical cloudiness reductions are associated with inversion strength anomalies originating from higher-latitude synoptic storms (*10*). Aircraft measurements off the coast of California show that near-shore clearings of the marine cloud field can be associated with synoptic-scale perturbations in the alignment and strength of the northeast Pacific ridge and concurrent mesoscale circulations along the California coast (*19*). These near-shore clearings expand during the day and contract toward the coast at night.

Propagating atmospheric gravity waves (buoyancy oscillations) can manifest as transitions from overcast to broken cloud conditions and from thicker to thinner clouds. A westward-moving diurnal atmospheric gravity wave originating over the heated, elevated terrain of the Andes modulates the liquid water path (LWP) in marine low clouds over the southeast Pacific (*20*–*22*). Intermittent atmospheric gravity wave trains originating from a disturbed subtropical jet can move equatorward into the southeast Pacific subtropical cloud deck, modulate the LWP, and reduce the cloud fraction during the day (*23*, *24*).

The characteristics of the southeast Atlantic cloud clearings are inconsistent with advection and the specific gravity-wave mechanisms documented in the southeast Pacific. The westward motion of the southeast Atlantic cloudiness transitions in an environment of prevailing southerly and southeasterly cloud-level winds and a persistent, large-scale stable layer topped by an inversion that can serve as a waveguide (*25*) strongly suggest that the cloud erosion is caused primarily by an atmospheric gravity wave rather than advection. Additionally, the combination of the direction of motion, the phase speed, and the timing characteristics of these wavelike phenomena over the subtropical southeast Atlantic differs from that of documented atmospheric gravity waves over the subtropical southeast Pacific. The westward-moving diurnal solitary wave over the southeast Pacific is associated with heating of elevated terrain and crosses the coast at about 1700 local time (*20*, *21*). This westward-propagating atmospheric gravity wave has a wavelength of ≈400 km, a phase

[1]Department of Marine, Earth, and Atmospheric Sciences, North Carolina State University, Raleigh, NC, USA. [2]ICF, Fairfax, VA, USA. [3]Department of Geography and Atmospheric Science, University of Kansas, Lawrence, KS, USA.
*Corresponding author. Email: seyuter@ncsu.edu

speed of 30 m s^{-1}, and a wave depth of 5 km. The northeastward-moving atmospheric gravity wave trains that emerge from a disturbed subtropical jet and propagate toward the coast of Peru (*23*, *24*) have wavelengths of 50 to 100 km, a vertical displacement of ≈400 m, and a phase speed of ≈15 m s^{-1}. The wavelength and vertical displacement of the >1000-km-long southeast Atlantic cloud-eroding waves are currently not known, though the phase speed is in the range of 8 to 12 m s^{-1} and evidence of waves with wavelengths of ≤10 km can be observed concomitantly with the cloudiness transitions (Fig. 1, E and G).

Throughout the year in the southeast Atlantic, we also observed small-scale propagating cloud wave trains moving toward the south, southwest, southeast, and east. Figure 4 and movies S5 and S6 show an example when overlapping cloud wave trains moved southeastward, southwestward, and eastward coincident with westward-moving cloud

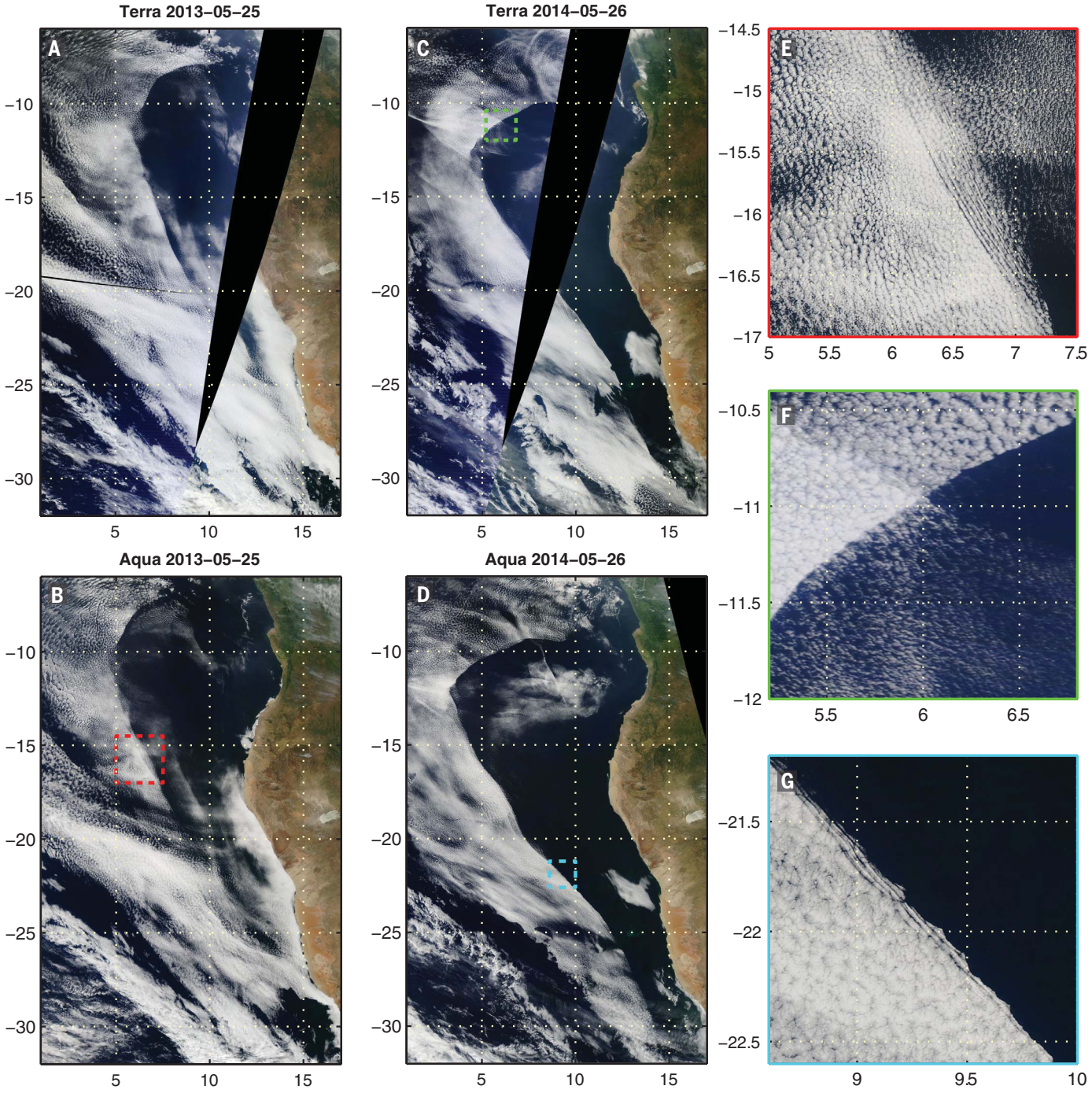

Fig. 1. Examples of westward-moving cloudiness transitions in the southeast Atlantic off the coast of Africa in MODIS corrected reflectance imagery. Consecutive pairs of Terra (≈10:30 a.m.) and Aqua (≈1:30 p.m.) images (**A** and **B**) on 25 May 2013 and (**C** and **D**) on 26 May 2014. (**E** to **G**) Boxed areas in (B) to (D) shown at greater magnification. Latitude and longitude grids are shown with dashed lines. Movie loop animations of the 26 May 2014 case are shown in movies S1 (reflectance) and S2 (IR).

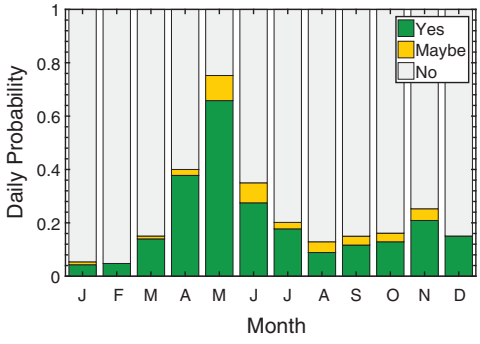

Fig. 2. Histogram of the daily probability of an abrupt cloudiness transition event occurring in a given month in the southeast Atlantic for the period from 8 May 2012 through 31 July 2017. For example, the 0.658 daily probability value for the "Yes" events category for May means that on average 20.4 of the 31 days of May have westward-moving cloud erosion boundaries over the southeast Atlantic. The analysis was performed on the basis of pairs of Terra (morning) and Aqua (afternoon) visible corrected reflectance images. See methods for details.

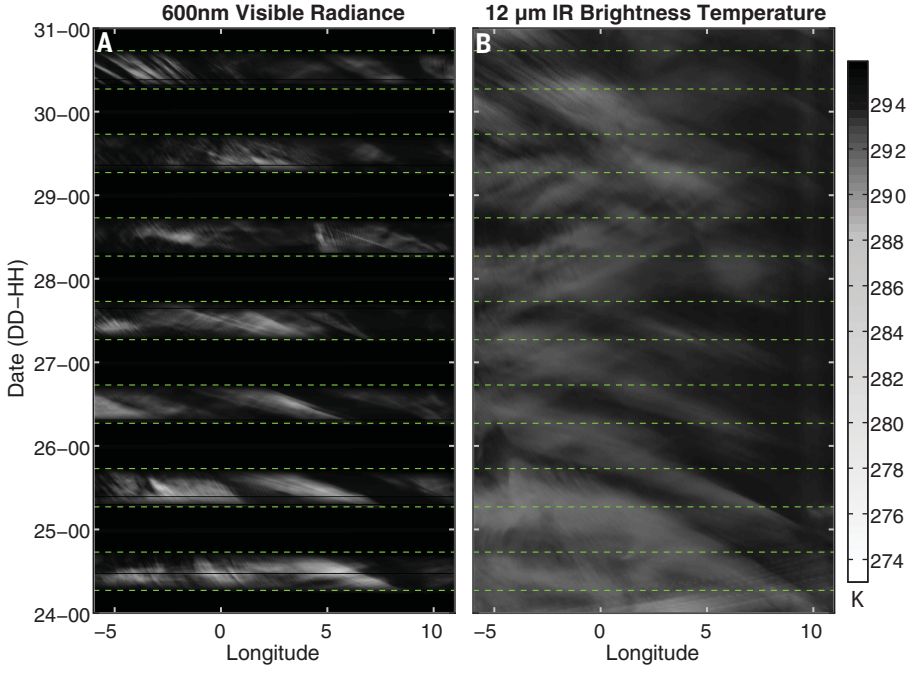

Fig. 3. Hovmöller plots illustrating cloud-clearing event timing and propagation speed. (**A**) Meteosat 600-nm visible imagery and (**B**) 12-μm IR brightness temperature from 00 UTC on 24 May 2014 to 00 UTC on 31 May 2014. The dashed lines denote the approximate sunrise and sunset times. Data are averaged meridionally over a box from 6°W to 11°E longitude and 12.5°S to 17.5°S latitude. DD, day; HH, hour.

erosion. Cloud wave trains associated with deep convective latent heating were documented off the northwest coast of Australia during seasons when deep convection was common over the nearby continent (*26*). A potential source for southward-moving atmospheric gravity waves in the southeast Atlantic is latent heating from tropical deep convection (*27*) over western equatorial Africa and from the Atlantic Intertropical Convergence Zone. The eastward-moving wave trains in the southeast Atlantic may originate from the disturbed subtropical jet, similar to cloudiness perturbations seen in the southeast Pacific (*23*).

Cloud generation by atmospheric gravity waves is extensively documented in the literature, and the associated physical mechanisms are reasonably well understood (*26, 28–32*) (see supplementary text for details). These studies show that when moisture and stability conditions are favorable, upward motions within the waves can yield propagating lines of clouds hundreds of kilometers in length moving on the order of 10 m s^{-1}.

By contrast, cloud-eroding waves defy easy explanation. The upward and downward motion associated with atmospheric gravity wave passage should yield reversible changes. For a parcel with a given temperature and specific humidity, upward motion decreases the temperature, increases relative humidity, and, if saturation occurs, can yield cloud. Downward motion increases temperature and decreases relative humidity. If the moisture content of the air is unchanged, cloudiness would increase with upward motion, decrease with downward motion, and return to the prewave cloud state once the wave passes through. Yet observations show that cloud erodes along the boundaries in an irreversible manner that yields a reduced cloud fraction for hours (movies S2 and S4).

For atmospheric gravity wave–induced cloud clearing to occur, a wave must be excited and then must propagate through a layer of the atmosphere that includes the top of the marine boundary layer where the clouds reside. Further, the wave needs to be associated with a localized mechanism that can irreversibly reduce the cloud fraction on time scales of tens of minutes. Lastly, the cloud deck itself must be susceptible to this erosion by the atmospheric gravity wave.

Why abrupt cloud clearing over the subtropical southeast Atlantic is most frequent in May is related to some combination of environmental conditions favoring the presence of the above-mentioned factors in the region and the season of interest compared with other seasons and regions. MODIS aerosol optical depth measurements show that abrupt cloudiness transitions occur in a variety of aerosol conditions (fig. S1). Comparison of large-scale conditions derived from the Modern-Era Retrospective Analysis for Research and Applications (MERRA) for May, the month with the most cloud erosion boundaries, and for January, the month with the fewest, indicates weaker stability in May than in January (a median estimated inversion strength of 4.3 K versus 5.1 K) but stronger subsidence (700-hPa vertical pressure velocity of 0.049 Pa s^{-1} versus 0.032 Pa s^{-1}).

Our hypothesis is that westward-moving atmospheric gravity waves cause the abrupt cloudiness transitions in the southeast Atlantic and are triggered by the interaction of offshore flow—likely combining a nocturnal land breeze and downslope winds from the coastal highlands (*33*)—with the stable marine boundary layer in a manner similar to processes that generate cloud-forming atmospheric gravity waves (*26*, *28*, *30*, *31*). For individual cloud erosion boundaries, we typically do not see evidence of slowing with increasing distance from the coast, as would be expected from a thinning, dissipating cold-air mass originating over land (Fig. 3). Among the three subtropical marine stratocumulus cloud decks in the northeast Pacific, southeast Pacific, and southeast Atlantic, the deck in the southeast Atlantic has the largest diurnal wind variability near the adjacent coast (*34*), which would be consistent with regular offshore flow events triggering gravity waves. Comparable westward-moving abrupt cloud-clearing events are not common in either the southeast Pacific or the northeast Pacific.

The removal of cloud over tens of minutes and the observation of bisected closed cellular cloud structures suggest a fast-acting mechanism. We hypothesize that cloud erosion is a consequence of rapid entrainment of warm and dry air from the free troposphere into the cloud layer by enhanced turbulence associated with a solitary wave train excited by offshore flow emanating from southwest Africa. Locally enhanced turbulent kinetic energy and mixing across the inversion

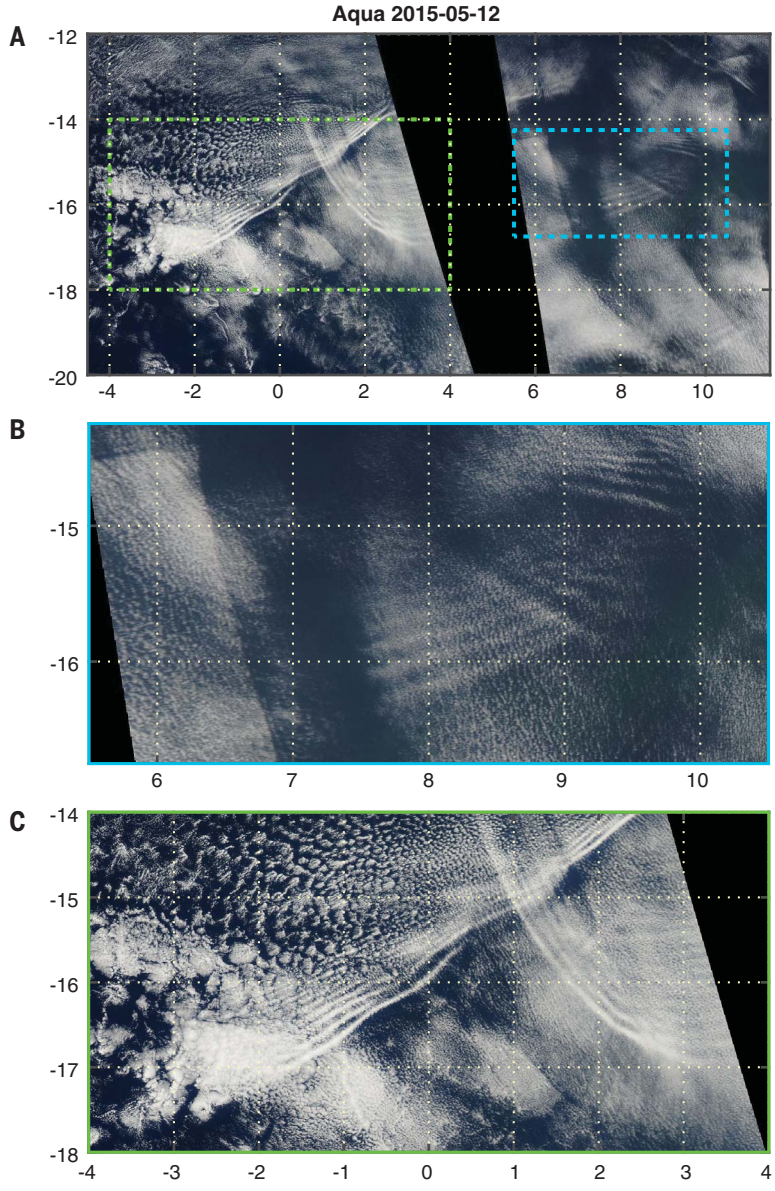

Fig. 4. Examples of multiple small-scale cloud wave trains propagating southeastward, southwestward, and eastward over the southeast Atlantic. MODIS corrected reflectance images centered off the west coast of Africa on 12 May 2015 during the afternoon Aqua overpass are shown. (**A**) Regional image with 2° grid lines. (**B** and **C**) Close-ups of waves overlaid with 1° grid lines corresponding to the inset boxes in (A). Movie loop animations of this case are shown in movies S5 (reflectance) and S6 (IR).

have been documented within a solitary wave packet in the central United States (*35*).

Targeted observations in the subtropical southeast Atlantic, including the use of dropsondes and airborne radar and lidar measurements, will be needed to resolve the mechanisms for rapid cloud erosion along cloud-eroding boundaries. The meteorological conditions associated with the formation and lack of formation of the cloudiness boundaries, as well as features of downslope winds and their interactions with the marine stable layer, are currently being investigated by combining observations, reanalysis, and mesoscale modeling.

Persistent, wide-area reductions in the cloud fraction over hundreds of kilometers associated with these westward-moving cloud erosion boundaries contribute to a lower March through May average cloud fraction in the subtropical southeast Atlantic than in any season in the subtropical southeast Pacific or the subtropical northeast Pacific (*36*). Mechanisms that yield substantial multiday variability in the marine stratocumulus cloud fraction are highly relevant to the climate system. Cloud-system resilience to external multiday perturbations and the frequency of these perturbations may be key factors in governing low-cloud variability and potential climate sensitivity.

REFERENCES AND NOTES

1. D. L. Hartmann, M. E. Ockert-Bell, M. L. Michelsen, *J. Clim.* **5**, 1281–1304 (1992).
2. C. S. Bretherton *et al.*, *Bull. Am. Meteorol. Soc.* **85**, 967–978 (2004).
3. W. H. Schubert, J. S. Wakefield, E. J. Steiner, S. K. Cox, *J. Atmos. Sci.* **36**, 1286–1307 (1979).
4. B. Stevens, *Q. J. R. Meteorol. Soc.* **128**, 2663–2690 (2002).
5. B. Stevens, W. R. Cotton, G. Feingold, C.-H. Moeng, *J. Atmos. Sci.* **55**, 3616–3638 (1998).
6. A. S. Ackerman *et al.*, *Mon. Weather Rev.* **137**, 1083–1110 (2009).
7. R. Wood *et al.*, *Atmos. Chem. Phys.* **11**, 2341–2370 (2011).
8. I. Sandu, B. Stevens, *J. Atmos. Sci.* **68**, 1865–1881 (2011).
9. A. H. Berner, C. S. Bretherton, R. Wood, A. Muhlbauer, *Atmos. Chem. Phys.* **13**, 12549–12572 (2013).
10. S. P. de Szoeke, K. L. Verlinden, S. E. Yuter, D. B. Mechem, *J. Clim.* **29**, 6463–6481 (2016).
11. C. Brunet, R. Casotti, V. Vantrepotte, *J. Plankton Res.* **30**, 645–654 (2008).
12. C. M. Risien, D. B. Chelton, *J. Phys. Oceanogr.* **38**, 2379–2413 (2008).
13. S. A. Klein, *J. Clim.* **10**, 2018–2039 (1997).
14. M. A. Rozendaal, W. B. Rossow, *J. Atmos. Sci.* **60**, 711–728 (2003).
15. R. C. George, R. Wood, *Atmos. Chem. Phys.* **10**, 4047–4063 (2010).
16. N.-C. Lau, M. W. Crane, *Mon. Weather Rev.* **123**, 1984–2006 (1995).
17. S. A. Klein, C. Jakob, *Mon. Weather Rev.* **127**, 2514–2531 (1999).
18. G. L. Stephens, *J. Clim.* **18**, 237–273 (2005).
19. E. Crosbie *et al.*, *J. Atmos. Sci.* **73**, 1083–1099 (2016).
20. R. Garreaud, R. Muñoz, *J. Clim.* **17**, 1699–1710 (2004).
21. C. W. O'Dell, F. J. Wentz, R. Bennartz, *J. Clim.* **21**, 1721–1739 (2008).
22. R. Wood, M. Köhler, R. Bennartz, C. O'Dell, *Q. J. R. Meteorol. Soc.* **135**, 1484–1493 (2009).
23. G. Allen *et al.*, *Q. J. R. Meteorol. Soc.* **139**, 32–45 (2013).
24. P. J. Connolly *et al.*, *Atmos. Chem. Phys.* **13**, 7133–7152 (2013).
25. S. A. Klein, D. L. Hartmann, *J. Clim.* **6**, 1587–1606 (1993).
26. C. E. Birch, M. J. Reeder, *Q. J. R. Meteorol. Soc.* **139**, 1311–1326 (2013).
27. B. E. Mapes, *J. Atmos. Sci.* **50**, 2026–2037 (1993).
28. R. H. Clarke, R. K. Smith, D. G. Reid, *Mon. Weather Rev.* **109**, 1726–1750 (1981).
29. D. R. Christie, K. J. Muirhead, R. H. Clarke, *Nature* **293**, 46–49 (1981).
30. F. Désalmand, A. Szantai, L. Picon, M. Desbois, *J. Geophys. Res.* **108** (D18), 8004 (2003).
31. J. C. B. da Silva, J. M. Magalhaes, *Int. J. Remote Sens.* **30**, 1161–1182 (2009).
32. P. A. Lutzak, *Weather Forecast.* **28**, 55–76 (2013).
33. T. Qian, C. C. Epifanio, F. Zhang, *J. Atmos. Sci.* **69**, 130–149 (2012).
34. S. T. Gille, *Geophys. Res. Lett.* **32**, L05605 (2005).
35. S. E. Koch *et al.*, *Mon. Weather Rev.* **136**, 1373–1400 (2008).
36. C. D. Burleyson, S. E. Yuter, *J. Clim.* **28**, 2968–2985 (2015).
37. J. Hader, "Propagating, cloud-eroding boundaries in southeast Atlantic marine stratocumulus," thesis, North Carolina State University, Raleigh, NC (2016).
38. NASA, EOSDIS Worldview; https://worldview.earthdata.nasa.gov/.
39. EUMETSAT Product Navigator, http://navigator.eumetsat.int/.
40. J. Janowiak, B. Joyce, P. Xie, NCEP/CPC L3 half hourly 4km global (60S - 60N) merged IR V1, A. Savtchenko, Ed. [Goddard Earth Sciences Data and Information Services Center (GES DISC), 2017]; http://dx.doi.org/10.5067/P4HZB9N27EKU.
41. S. E. Yuter, Southeast Atlantic westward-moving cloud erosion boundaries, Open Science Framework (2018); doi:10.17605/OSF.IO/KR4JS.

ACKNOWLEDGMENTS

M. T. Bryant, E. S. Chan, L. Lovell, S. Rhodes, E. Scott, and L. Tomkins helped to analyze satellite data. **Funding:** This work was supported by U.S. Department of Energy grants DE-SC0006701, DE-SC0006736, and DE-SC0016522 and NSF AGS grants 1656237 and 1656314. **Author contributions:** All authors contributed to the formulation of the conceptual model, analysis design, interpretation of the data, and critical

revision of the article. J.D.H. performed the majority of the data acquisition and processing, with M.A.M. aiding in these efforts. S.E.Y. drafted the article, in part on the basis of J.D.H.'s thesis (*37*). **Competing interests:** None of the authors have competing interests. **Data and materials availability:** Satellite datasets used in this study are archived and accessible at https://worldview.earthdata.nasa.gov/, http://navigator.eumetsat.int/discovery/Start/DirectSearch/DetailResult.do?f(r0)=EO:EUM:DAT:MSG:HRSEVIRI, and https://disc.gsfc.nasa.gov/datasets/GPM_MERGIR_V1/summary?keywords=GPM_MERGIR_1 (*38*–*40*). Dates and times for the 377 southeast Atlantic westward-moving cloud erosion boundaries are accessible at Open Science Framework (*41*).

SUPPLEMENTARY MATERIALS

www.sciencemag.org/content/361/6403/697/suppl/DC1
Materials and Methods
Supplementary Text
Fig. S1
Table S1
References (*42*–*56*)
Movies S1 to S6

24 November 2017; accepted 8 July 2018
Published online 19 July 2018
10.1126/science.aar5836

Abrupt cloud clearing of marine stratocumulus in the subtropical southeast Atlantic

Sandra E. Yuter, John D. Hader, Matthew A. Miller and David B. Mechem

Science **361** (6403), 697-701.
DOI: 10.1126/science.aar5836originally published online July 19, 2018

A shrinking marine refrigerator

Low subtropical marine clouds scatter solar radiation back to space and thereby cool the climate system. Most work on understanding changes in the coverage of these types of clouds has focused on the effects of sea surface temperatures or on aerosols. Yuter *et al.* show that dynamic effects due to atmospheric gravity waves are responsible for the rapid clearing of large areas of these clouds. This phenomenon also has implications for marine ecology and biogeochemistry.

Science, this issue p. 697